Sustainable Energy & Fuels

ROYAL SOCIETY OF CHEMISTRY

PAPER

View Article Online
View Journal

Cite this: DOI: 10.1039/d4se00731j

Choosing a liquid hydrogen carrier for sustainable transportation†

Athanasios A. Tountas, [a] Geoffrey A. Ozin *[b] and Mohini M. Sain [ac]

Liquid hydrogen carriers (LHCs) are important shuttles for molecular hydrogen (H_2) as they are convenient to transport as energy-dense liquids over distances greater than 10 000 km. Herein, we provide comprehensive insights into the comparative practicality and safety of irreversible LHCs. From a gas purification standpoint, fewer products in the released H_2 stream result in less separation complexity and lower cost. Unit operational complexities of methanol (MeOH) steam reforming *versus* fossil steam-methane reforming were analyzed in depth to highlight gas-cleaning complexities. The main challenge is to estimate the costs of LHC reforming, cleaning and compression (RC&C) steps for H_2 production in order to break even with other energy scenarios. To achieve this, two techno-economic analyses (TEA) were performed from the 'vehicle' and 'fuel' points of view. 'Vehicle' analysis compares the use of MeOH-to-H_2 for proton-exchange membrane fuel-cell vehicles (FCVs) with the use of MeOH directly as drop-in fuel for conventional vehicles (ICEVs). 'Fuel' analysis compares renewable MeOH and dimethyl ether LHC transport with pressurized and cryogenic H_2 transport for FCVs. For the analyses in which H_2 gas is produced as a fuel, RC&C steps are assumed to be accomplished off-board or before fueling the vehicles. 'Vehicle' analysis findings indicate that with a moderate tax on carbon emissions, in the year 2035 and beyond, FCVs can be competitive with ICEVs with an RC&C cost of ~US $ 2–6 per kg H_2. From the 'fuel' analysis perspective, LHCs break-even with gaseous and liquid H_2 transport at a more flexible RC&C cost of US $ 7.9–11.4 per kg H_2.

Received 31st May 2024
Accepted 2nd September 2024

DOI: 10.1039/d4se00731j

rsc.li/sustainable-energy

1. Introduction

Former U.S. President George W. Bush, in his State of the Union Address in January 2003, made perhaps the first public endorsement for the hydrogen (H_2) economy as a compelling future vision in which fuel exhaust would consist solely of water vapor.[1] Only in the past few years has technological progress caught up with the business case for H_2 around logistics, storage, and commercial niches. These niches include long-haul transport, shipping, and aviation sectors, where energy-to-weight or -volume ratios and rapid refueling are paramount, despite the ever-improving convenience and rapid-deploying infrastructure of light-duty fully electric vehicles. Electrifying heavy-duty vehicles with current technology would necessitate megawatts of power charging infrastructure and long wait times at fueling stations with current Li-based batteries. Furthermore, batteries have much further to go in terms of technological maturity to meet a range of requirements, including high energy density, high power density, many life cycles, environmental friendliness, robustness, durability, safety, and low cost.[2] Another often overlooked sector is power generation and storage, where H_2 could foreseeably replace natural gas (NG) as grids de-fossilize since it is already considered a carbon-free fuel alternative for consumer home heating.

Liquid hydrogen carriers (LHCs) are imperative to effectively shuttle renewable H_2 from energy-rich to energy-poor regions. Economically justifiable deployment of extensive photovoltaic and wind turbine capacities requires mid-to equatorial latitude regions with above-average solar insolation (kW h m^{-2}) and wind corridors with abundant wind supply, respectively. If shuttling H_2 to markets is the goal, generated renewable H_2 can either be chemisorbed (*via* metal hydrides) or physisorbed (*via* carbon nanotubes or metal–organic frameworks) or transformed *via* power-to-gas or -liquid processes and stored in chemical bonds as in LHCs.[3] LHCs and liquid H_2 allow energy-dense transport by tanker trucks, pipelines, and ship infrastructures, and the former can be stored in low-cost tank farms. Thirty-seven renewable-energy-rich countries with strong export potential have been identified, including Morocco and Namibia, which are planning to spend or have already earmarked ~tens of US $ billions for generating green H_2.[4–6] They are, however, situated at remote distances from population centres.

[a]Department of Chemical Engineering and Applied Chemistry, University of Toronto, 200 College St., Toronto, Ontario, M5S 3E5, Canada

[b]Department of Chemistry, University of Toronto, 80 St. George St., Toronto, Ontario, M5S 3H6, Canada. E-mail: g.ozin@utoronto.ca

[c]Department of Mechanical and Industrial Engineering, 5 King's College Road, Toronto, Ontario, M5S 3G8, Canada

† Electronic supplementary information (ESI) available. See DOI: https://doi.org/10.1039/d4se00731j

Table 1 Select properties of LHCs

Process	Reaction equation	Stoichiometric H_2 per carrier (mol mol^{-1})	$\Delta H_{R,298K}$ Reaction energy per carrier (kJ mol^{-1})	$\Delta H_{R,298K}$ Reaction energy per produced H_2 (kJ mol^{-1}) (ranked by)[a]	Feed gas (vol : vol%)	Reaction conditions T (°C), P (bar)	Reforming energy to H_2 lower heating value (LHV) (%)	CO_2 produced per H_2 product (kg CO_2 per kg H_2)	Water demand per H_2 product (kg H_2O per kg H_2)
H_2 liquefaction	$H_2(g) = H_2(l)$	1	Na	65.3	Na	−253, 1	18–30 (liquef. energy)	Na	Na
Water splitting	$H_2O(l) = H_2 + \frac{1}{2}O_2$	1	241.8	241.8	Pure H_2O	≤100, ≥1	100.0	0.0	8.9
Steam-methane reforming (SMR)	$CH_4 + 2H_2O = CO_2 + 4H_2$	2	165.0	41.3	1 : 2.5–3 CH_4 : H_2O[9]	800–900, ≤30 Supported-Ni catalyst[9]	17.1	5.5	4.5
Ammonia decomp	$NH_3(g) = \frac{1}{2}N_2 + 3/2H_2$	1.5	45.6	30.4	Pure NH_3	400, ≥1 (eqm. 99% conv.[d])	12.6	0.0	0.0
Ethanol steam reforming (ESR)	$CH_3CH_2OH + 3H_2O = 2CO_2 + 6H_2$	3	173.1	28.9	1 : 3 EtOH : H_2O	400–800, ≥1 [10]	11.9	7.3	4.5
DME steam reforming (DSR)	$CH_3OCH_3(g) + H_2O(g) = 2CH_3OH$ $2CH_3OH(g) + 2H_2O(g) = 2CO_2 + 6H_2$	3	135.0	22.5	1 : 1 DME : H_2O	200–350, ≥1 [11]	9.3	7.3	4.5
MeOH steam reforming (MSR)	$CH_3OH(g) + H_2O(g) = CO_2 + 3H_2$	2	49.6	16.5	1 : 1 MeOH : H_2O	200–250, ≥1 (eqm. 99% conv.[d])	6.8	7.3	3.0
MeOH decomp. + water–gas shift (WGS) (staggered)	$CH_3OH(g) = CO + 2H_2$ $CO + H_2O(g) = H_2 + CO_2$	2	49.6	16.5	1 : 1 MeOH : H_2O	WGS HTS[b]: 310–450, 1–10 [12] WGS LTS[c]: 200–250, 1–10	6.8	7.3	3.0

[a] Produced H_2 is the H_2 released from the reforming reaction stoichiometry; note that it can be derived from water as a co-reactant. [b] Water–gas shift high-temperature step. [c] Water–gas shift low-temperature step. [d] From Aspen Plus V10 (Fig. 1).

To address the remoteness, Namibia is poised to produce and export 2 million metric tonnes of ammonia by 2030.[7] Due to political and other factors, many global export routes are desirable to avoid dependency on any one nation. As will be discussed, transporting H_2 *via* tanker ships over global distances at or above 10 000 km, or $\frac{1}{4}$ of the earth's circumference, benefits from LHC intermediates.

H_2 derivatives or irreversible carriers are those that require external regeneration infrastructure or significant chemical reconstitution after releasing their stored H_2.[4] In contrast, reversible carriers are those that can be regenerated in place or without significant chemical reconstitution after releasing their stored H_2. Irreversible carriers include methane (liquid at 4.6 MPa and −82 °C), ammonia (liquid at 0.75 MPa and 20 °C or 0.1 MPa and −50 °C), methanol (MeOH) and ethanol (EtOH) (both liquid at 0.1 MPa and 20 °C), and dimethyl ether (DME) (liquid at 0.52 MPa and 20 °C or 0.1 MPa and −15 °C), while the reversible carriers include at least a dozen chemical classes ranging from ethane-ethylene, branched aromatics, lithium hydrides, and silicon-based nanoparticles to borane compounds.[8] Although water itself contains H_2 and can be considered an LHC, it is omitted here as it is usually split at the source where renewable electricity is available and transported as lighter H_2. Table 1 notes water splitting for completeness. The challenge of transporting reversible H_2 carriers over a considerable distance is their comparatively low gravimetric (by mass) and volumetric (by volume) H_2 content relative to irreversible LHCs (see Fig. 1A).

It has been estimated that using regional H_2 pipelines (*e.g.* in the E.U. region) is more cost-effective (H_2 transportation cost of US $ 0.18 per kg per 1000 km in 2021 dollars) than shipping LHCs (excluding ammonia), ammonia, or liquid H_2 (from more to less economical) across distances up to around 10 000 km, beyond which shipping LHCs (excluding ammonia) becomes more economical.[13] At present, the NG pipeline infrastructure cannot accommodate more than a certain concentration of gaseous H_2 (approximately 15% H_2), beyond which H_2 embrittlement may begin to affect piping networks.[14] The cost to convert existing pipeline networks to transport H_2 would include modifying compressors, seals, measuring devices, and liners, and research is ongoing to assess if the costs are reasonable or prohibitive and whether it is an efficient use of public and private funds.[14] Furthermore, the low ignition energy of H_2 (0.021 mJ or a small fraction of static discharge) and ignition of H_2 plumes from leaks can cause overpressures exceeding NG, causing potentially extensive and costly damage, and therefore needs to be adequately managed.[13,15]

Conversely, existing NG, crude oil, or refined oil product infrastructure could be more cost-effectively modified to accommodate alternative, renewable, energy-dense gases and liquids. Similarly, liquefied petroleum gas (*e.g.* butane and propane) has similar properties to DME, whereby the existing network infrastructure could be immediately utilized.[16] It has also been noted that the existing NG infrastructure is suitable for distributing DME.[17] The vast accumulated financial investment in the existing pipeline infrastructure (in the US $ trillion range in North America) emphasizes the need to maximize its use.[18] If carbon dioxide (CO_2) used in the H_2 carrier creation process (*e.g.* for methanation or MeOH or DME synthesis) is captured from the atmosphere cyclically or harvested from a biogenic source (*e.g.* biogas, waste, or agriculture and forestry products for example), minimal or no net CO_2 emissions will result. The flexible use of MeOH or DME for fine-chemical production will additionally provide a renewable de-fossilized carbon source for society.[19] In a recent forum at the World Hydrogen Week in Rotterdam (Oct. 2023), MeOH's role as an

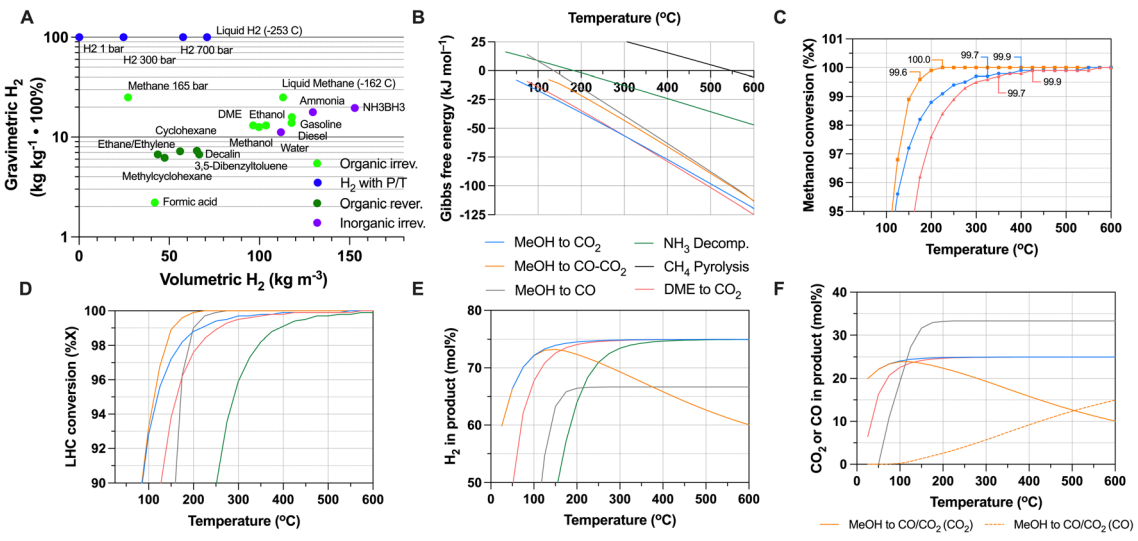

Fig. 1 Thermodynamic evaluation of LHCs: (A) a comparison of gravimetric and volumetric energy densities for both reversible and irreversible H_2 carriers compared to H_2, with all quantities in terms of useable H_2 (including H_2 from water when steam reformed); (B) Gibbs free energy of reforming reactions as a function of temperature for various irreversible LHCs; (C) thermal equilibrium conversion extents of MeOH and DME LHC steam-reforming reactions; (D) thermal equilibrium conversion extents of several more LHC reactions; (E) product gas H_2 composition of several LHCs; (F) product gas carbon-containing composition of several LHCs. Note that (A) is from densities and molecular weights and (B–F) are all H_2-releasing reactions of LHCs from the Aspen Plus analysis conducted herein. All reactions are considered at ambient pressure.

LHC was discussed as an important carbon source and building block for jet fuel and plastic production, while ammonia was seen as a carbon-free carrier and fertilizer that requires a larger investment in infrastructure and technology if used as an H_2 carrier.

The top five important sectors for the potential application of H_2, ranked by global emissions (2019), are electricity and heat production (34%), industry (24%), agriculture, forestry, and other land use (22%), transportation (15%), and buildings (6%).[20] Besides battery-electric vehicles for transportation, renewable H_2 will likely be used in proton-exchange membrane fuel-cell vehicles (FCVs) that continue to advance in terms of lowering precious metal content and increasing durability.[21] The U.S. Department of Energy (U.S. DOE) has stated that on-board mobile reforming (along with a few other technologies, including the hydrolysis of aluminium metal and alloys) is unlikely to achieve performance targets of capacity (gravimetric and volumetric), cost, durability, operability, or charging or discharging rates.[22] Therefore, the focus herein is on releasing the stored H_2 in LHCs *via* stationary reformers.

We are focused on the gas-phase heterogeneous H_2-releasing reactions of LHCs since gas-phase reaction methods are recognized to produce 10-fold more H_2 reaction activity than liquid-phase homogeneous reactions, due to reduced competition for water at absorption sites.[23] It is equally beneficial that heterogeneous reactions are high-throughput, scalable, and already in use industrially for many chemical syntheses. The final cost of H_2 fuel at the pump is critical when discussing renewable fuels. The 2026 U.S. DOE 'ultimate' (or final in a progression) PEM electrolysis H_2 production targets are US $ 1.00–2.00 per kg or gasoline gallon equivalent (gge), where a kilogram of H_2 is equal to a gge. The 2020 'ultimate' H_2 delivery targets were US $ 1.70–2.15 per kg making the target final H_2 cost of US $ 2.70–4.15 per kg.[24,25]

2. Methods of identifying a promising LHC for transportation

2.1 Objectives of this study

In this study, we have investigated transportation fuelling alternatives to gaseous- and liquid-H_2, *i.e.*, liquid carriers that can be stored long-term under near ambient conditions. Although other researchers have investigated the economics of long-distance H_2 carriers (MeOH, ammonia, and DME),[26] they do so from an energy demand point of view (shipping, reforming/cracking, and liquefaction energy demand) and perhaps overlook the stringent gas-purification requirements for technical FCV-compatible H_2, and multi-step cleaning and conditioning requirements, of the reforming, cleaning, and compression (RC&C) steps that we believe are the cost bottlenecks for an economically viable H_2 value chain. Further, we examined the direct use of LHCs (analogous to the fuelling convenience of fossil fuels) in existing internal combustion engine vehicles (ICEVs), which will require public persuasion to adopt the efficient use of LHCs in FCVs through a gradually increasing tax on greenhouse gases.

We begin in Section 3 with an initial LHC screening that involves a high-level comparison of LHCs, for the expert and non-expert alike, to set the stage for the rest of the analysis. This includes a comparative LHC-reforming thermodynamic analysis to highlight subtle differences when examining the spectrum of available LHCs side by side.

Section 4 provides a brief discussion of catalytic reforming options where we highlight the thermal-reforming *vs.* photo-reforming of LHCs, with a focus on why low-temperature reforming is the future from a gas cleaning perspective. This includes the examination of the added benefits of choosing the right feedstock for sourcing H_2, either from LHCs or NG.

In Section 5, we conclude with two techno-economic (TEA) analyses of the RC&C cost from the 'vehicle' point of view for FCVs *vs.* ICEVs, and from the 'fuel' point of view for LHCs *vs.* gaseous- and liquid-H_2 transport for FCVs.

The results are summarized and the impact of the study is presented in the concluding section.

3. Initial LHC screening

3.1 High-level LHC comparison

Table 1 lists several key LHCs: methane, ammonia, MeOH, and DME, ranked by the reaction energy required to release produced H_2 (kJ mol^{-1}), along with liquefied H_2 for comparison. Pertinent data is also shown associated with reforming conditions and net energy requirements. Fig. 1A supplements this table, which shows the two most important metrics for LHC transportation: the gravimetric and volumetric H_2 carrier densities, which convey the cargo volume needed to transport a given mass. Interestingly, of the irreversible organic and inorganic H_2 carriers, ammonia borate and liquid ammonia rank the highest for these metrics, followed by liquid methane, gasoline and diesel hydrocarbons, EtOH, MeOH, and finally, DME. Ammonia borate has attracted significant research interest in the past due to its excellent capacity (gravimetric H_2 density of 0.196 kg H_2 per kg and volumetric H_2 density of 152.8 kg m^{-3})[8,15] but remains problematic to regenerate. Reversible carriers, including ethane-ethylene, and aromatic carriers such as cyclohexane, methylcyclohexane, decalin, 3,5-dibenzyltoluene, and similar compounds, rank lower in these metrics (Fig. 1A).[15,27] Although aromatic precursors such as benzene, toluene, and xylene are plentiful by-products of oil refining and their hydrogenation and dehydrogenation have been extensively carried out at scale, their low gravimetric H_2 content (<8 wt%) make their transport more costly than irreversible LHCs, especially in the context of global distances.[15] Reversible LHCs such as dibenzyl- and benzyl-toluene may be more practical for regional transport (*i.e.* distribution to filling stations).[15] Nonetheless, their volatile nature (odour perceived at filling stations) and links to adverse health effects such as leukaemia and other hematopoietic cancers (benzene and ethylbenzene) and adverse reproductive effects (toluene and xylene) should be prudently deliberated.[28] The organic carrier formic acid ranks lowest in terms of the gravimetric H_2 density of all the carriers considered here, and it is limited by being a highly corrosive liquid at room

temperature but more importantly, in high concentrations, it has a limited shelf-life on the order of months to a year.[29]

3.2 Thermodynamic simulation results and analysis

3.2.1 Aspen simulation parameters. This section details the comparative thermal-equilibrium reforming characteristics of several LHCs using the Aspen Plus V10 software. The non-random-two-liquid property package was chosen because it is suitable for low pressures typical of reforming processes. A temperature range analysis was performed using the equilibrium reactor, where the reactions of interest (reactants and products) were specified. Typically, pure streams of reactants were fed into the reactor to approximate commercial systems, and atmospheric pressure was chosen to account for Le Chatelier's principle. In practice, the reforming pressure may better match the gas cleaning pressures to minimize compressing hot gases. Inlet flows were specified at 1 kmol h^{-1}, and product mole fractions and conversions were calculated on this basis.

3.2.2 Thermal equilibrium study results. As can be seen in Fig. 1B, the thermal Gibbs free energy of the reaction is negative (or the reaction is spontaneous) for the MeOH and DME dehydrogenation reactions under the mildest conditions, which limited the formation of FCV-poisoning carbon monoxide (CO), favoured at higher temperatures. Favourable spontaneity at low temperatures resulted in lower energy-input-per-mol H_2 produced. Compared to splitting liquid water, DSR was an order of magnitude less energy-intensive (see ranked column Table 1) but some precursor H_2-generation step was necessary for DME formation. The unfavourable nature of the ammonia decomposition and SMR reactions is also worth noting, which required a minimum temperature of ~200 °C to 550 °C to become spontaneous.

In Fig. 1C, the temperatures and conversion relationships of MSR and DSR are specifically shown, with MeOH-to-CO and CO_2 being the most favored followed by MeOH-to-CO_2 and DME-to-CO_2. They each attained 99.9% conversion at 200 °C, 400 °C, and 425 °C, respectively. As can be seen in Fig. 1D, the conversion of ammonia *via* thermal decomposition required a temperature of 575 °C to achieve the same conversion as MSR or DSR. Ammonia conversion was only 99.4% at the temperature that DME achieved 99.9%.

This analysis shows that the ether group of the DME molecule behaved thermodynamically similar to the hydroxyl group of MeOH. It should be noted that EtOH reforming was not overlooked as it produces the same quantity of H_2 as DME; however, it requires ~25% more energy to reform (Table 1) at temperatures upwards of 400 °C to 800 °C due to the strong C–C bond.[10] However, EtOH reforming was still of interest due to its environmental benignity and low negative health effects on humans.[30]

3.2.3 By-product generation analysis. In Fig. 1E, MeOH, DME, and ammonia produced identical high-H_2-concentration product gas. In the case of MSR where the catalyst allowed for the formation of both CO and CO_2, the amount of CO_2 decreased monotonically after peaking near 125 °C, and CO conversely increased. Ideally, if CO formation could be hindered, the gas clean-up requirements would decline and become less complex; however, this would be at the expense of the maximum achievable theoretical conversion (Fig. 1C). MeOH decomposition produced a 2 : 1 mixture of H_2 : CO, which may be more cost-effectively purified, although further H_2 production would require a tandem one- or two-step WGS process. Aspen Plus was also used to evaluate the onset of spontaneous DME decomposition, forming CO, CO_2, H_2, CH_4, H_2O, and MeOH by-products. This necessitated high temperatures (~400 °C to 500 °C) and resulted in a complex-equilibrium gas-product mixture (~2 : 10 : 13 : 14 : 61 mol% H_2O : H_2 : CO : CO_2 : CH_4) and was thus omitted going forward.

Fig. 1F shows the carbon-containing compounds in the product gas and thus indicates the required degree of gas purification. MeOH and DME conversions primarily to the CO_2 by-product were the least complex cases and are, therefore, favourable for low-temperature research. Ammonia avoided carbon by-products but required the removal of N_2 that can be vented directly to the atmosphere without concern.

3.2.4 Social and environmental analysis. The ideal carrier should be non-toxic to humans and exhibit benign environmental effects in case of spillage (which limits MeOH and ammonia), it should also be non-corrosive or have non-detrimental effects on existing infrastructure (which limits high-concentration ammonia), and low global-warming potential (which limits methane $GWP_{100\ years,methane}$: 27–30). Further, it should have low alternative competing uses (which limits ammonia *e.g.* for fertilizer, and water *e.g.* for food, agriculture, and consumption), and low feed purity requirements (which limits water: *e.g.* high purity is needed for PEM electrolysis cells). Accounting for these considerations results in carrier candidates such as DME and EtOH, with the former having lower reforming energy to released H_2 LHV (9.3 *vs.* 11.9%) as per Table 1. It should be noted that the technologies exist to utilize ammonia today; however, its toxicity, flammability, corrosiveness, energy demand (12.6% reforming energy to released H_2 LHV), and unpleasant odour complicate its use.[15] It is also important to note that industrial-grade ammonia (27 wt% NH_3) is diluted with balanced water for safe handling. Research continues into alternative ammonia-based compounds such as ammonium carbamate or carbonate, urea, ammonium formate, ammonium metal complexes, and others to explore easier dissociation and safer handling pathways.[15]

DME, which satisfies all the above requirements, is non-toxic to humans, can be stored near densely populated urban areas with little cause for concern, and has low environmental persistence ($GWP_{100\ year,DME}$: 0.3). Perhaps the only moderate drawback of DME is the need for fresh water to catalytically dehydrogenate it (~4.5 kg H_2O per kg H_2, see Table 1) at the destination. The other carriers that require fresh water are methane (same quantity as DME) and MeOH (~3.0 kg H_2O per kg H_2), while ammonia avoids water altogether.

Freshwater management will continue to be key in the future as it has been estimated that the average person needs 70 times as much water to feed them than for all domestic purposes (the latter typically being 20 L per day to 50 L per day in developed countries).[31] Another challenge is the renewable electricity

demand to produce LHCs, with estimates of MeOH production requiring ~10–11 MW h_{elec} per mt MeOH and DME requiring ~18 MW h_{elec} per mt DME, with the former range being comparable to the annual electricity consumption of a typical U.S. household (2021).[3,32,33] DME is typically synthesized *via* dehydrating two MeOH intermediates, starting with two steps (syngas → 2MeOH → DME + H_2O) or with syngas in one step (syngas → DME + H_2O). It can also be synthesized from CO_2 but at a lower equilibrium yield in traditional processes.

Using MeOH or DME as drop-in fossil-fuel replacements is still a higher cost (4- to 5-fold) option due to their H_2 requirements, and thus more efficient ways to use these carriers are necessary, such as carrier → H_2 → fuel for FCVs, or carrier → jet fuel or fine chemicals.[32,34] Affordable renewable electricity will be key to larger market penetration of electricity-derived fuels or e-fuels.

MeOH will, nevertheless, be considered in parallel with DME in the subsequent economic analysis as it is easily interconvertible to DME with today's technology. Furthermore, the direct use of MeOH offers significant energy savings compared to DME.

4. Discussion of catalyst and feedstock options

4.1 Catalytic reforming options

Low-temperature reforming processes translate into lower CO and other harmful byproducts that can be detrimental to FCV catalysts. Furthermore, a less complex product mixture can generally aid in reducing the complexity of gas cleaning.[35] The CO threshold outlined in ISO 14687-2 fuel-cell H_2 specification is ~0.2 ppmv (Table 2).[37] Thus, low-temperature methods such as photocatalysis for accelerating or intensifying reforming reactions without added heat are becoming increasingly relevant, where CO-forming reactions are kinetically hindered or slowed. Another promising approach to achieve high conversion at low temperatures is to use *in situ* membrane separation of H_2, which shifts the equilibrium favourably to products. These processes can combine reforming, WGS, and H_2 separation in one step.[38] Decoupling the H_2 production rate from temperature to light intensity or tunable wavelengths remains a vision for photoreforming that could result in simplified gas cleaning complexity while allowing for more long-term catalyst stability and flexible production conditions. Finally, both thermal and photothermal catalytic options would benefit from catalysts that operate at near stoichiometric water demand instead of high water-to-LHC ratios to reduce the energy demand for steam generation and heating.[26]

4.1.1 Thermal catalysts. Many thermal catalyst systems have been proposed for MSR, as covered here.[16,39] Typically, a good MeOH synthesis catalyst would also act as a good steam-reforming catalyst under lower space velocity conditions. However, the traditional copper-based copper-zinc oxide-alumina catalyst, used successfully for decades for MeOH synthesis, presents challenges due to its short-lived stability under MSR conditions.[40] Catalysts based on Pd and ZnO that avoid the dispersed copper phase have shown improved durability under operating conditions and exhibit low CO selectivity.[39,41]

Another approach highlighted earlier is to directly decompose MeOH into CO and H_2 on a standalone Pd catalyst and shift the CO out of the system in the downstream WGS step(s). This approach has not been extensively documented. Thermal DSR catalysts have been documented, with all except one in the >300 °C operating range.[16] In an equilibrium analysis carried out by researchers at Los Alamos National Laboratory, they identified that the optimal thermodynamic DSR conditions were at a steam-to-carbon ratio of 1.5 with a pressure of 1 bar and a temperature of 200 °C to maximize H_2 (0.72 effluent mol fraction) and minimize CO.[17] It was also found that increasing the reforming pressure from 1 to 5 bar decreased the H_2 production efficiency by 12%. Finally, they showed that the equilibrium-limited step in DSR was the hydrolysis of DME to

Table 2 | ISO 14687-2 H_2 maximum impurities for H_2 fuels cells, Type I & II Grade D (99.97% H_2, total non-H_2 gas 300 ppmv).[36]

Component	Water	Total hydrocarbon compounds as methane basis	Oxygen	Helium	Nitrogen	Argon	CO_2
Maximum impurity concentration (in ppmv, unless stated otherwise)	5	2	5	300	100	100	2

Component	CO	Total sulphur compounds	Formaldehyde	Formic acid	Ammonia	Total halogenated compounds	Particulate concentration
Maximum impurity concentration (in ppmv, unless stated otherwise)	0.2	0.004	0.01	0.2	0.1	0.05	1 mg kg^{-1}

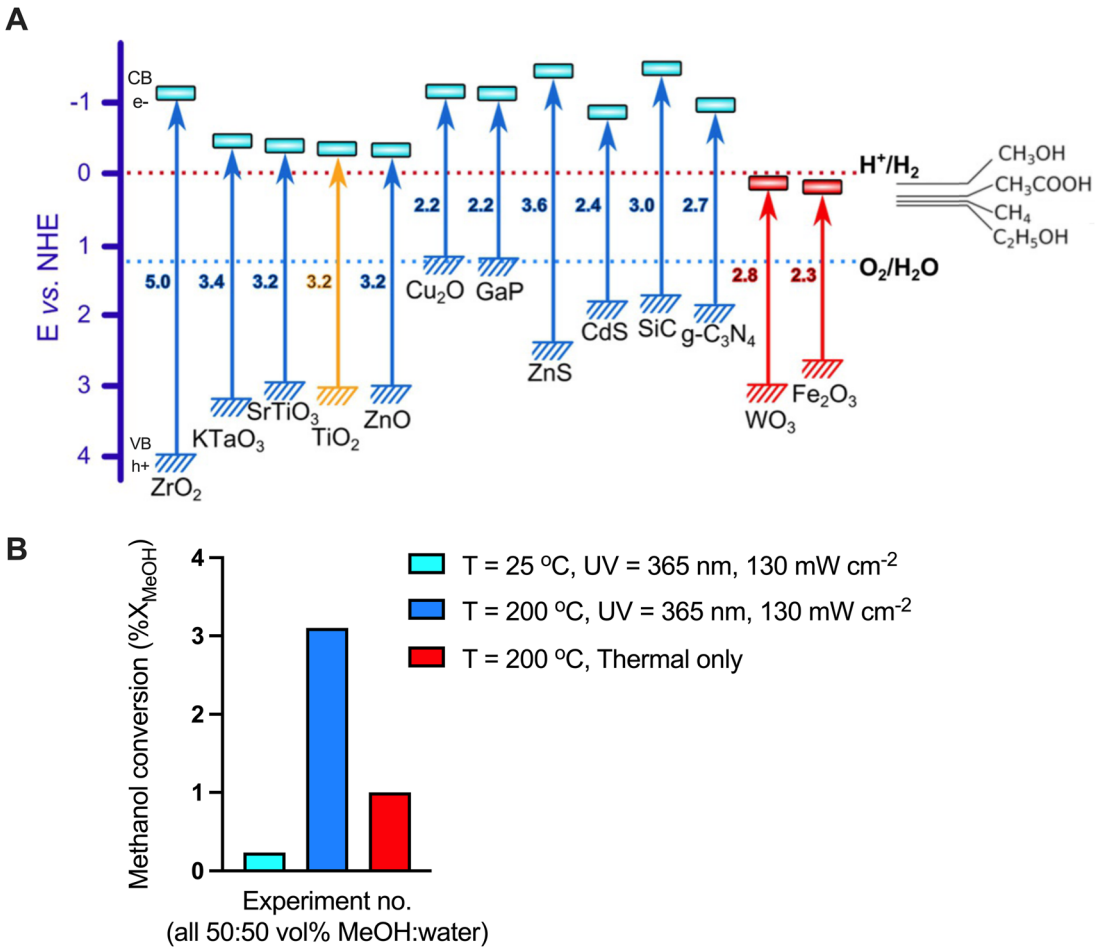

Fig. 2 Photocatalytic dehydrogenation: (A) band gap energies and band positions of photoactive semiconductors, and oxidation potentials of a few LHCs compared to water splitting ($H_2O \rightarrow H_2 + \frac{1}{2}O_2$);[23] (B) ZnO catalyst for MSR in a batch reactor (author's work) showing percent MeOH conversion (% X MeOH) at conditions of a 50 : 50 MeOH : water vol% ratio, 60 psig, for 20 min (single measurement each).

MeOH that had maximum thermal conversion and yield as the steam : DME ratio increased.

4.1.2 Photocatalysts. Photo-reforming is a promising research area that uses photons to intensify reforming activity under less severe thermal conditions. In the literature, the topic of photo-reforming LHCs has been somewhat confusingly covered as a form of scavenger-assisted water-splitting where LHCs serve as sacrificial agents for the photogenerated holes (h^+).[16,23,42,43] Fig. 2A shows that after a photon has been absorbed, it creates an electron and hole pair in which the electron has been excited from the valence band to the conduction band of the semiconductor photocatalyst. Next, the generated electron (e−, reducing agent) energy must be more negative than the H^+/H_2 potential (*y*-axis of Fig. 2A), and the hole (h^+, oxidizing agent) energy must be more positive than the O_2/H_2O potential. In practice, however, the oxygen evolution reaction is the main bottleneck of water-splitting because the ∼1.23 eV theoretical potential effectively becomes 2.0 eV to 2.4 eV due to the kinetic overpotentials needed and the energy losses required to drive that reaction. LHCs offer a larger potential difference (∼0.08 eV) compared to the holes (h^+) than the thermodynamically unfavorable O_2/H_2O reaction (∼2.2 eV), and thus, LHCs can act as a more effective hole scavenger in water splitting. In practice, gas-phase heterogeneous photochemistry depends on the properties of the catalyst such as defects, diffusion, adsorption, dissociation, reaction (excited-state-free-energy reaction profile), and desorption processes, which are distinct from aqueous phase models.[44] However, gas phase heterogeneous redox reactions can be thought of analogously if one corrects the aqueous redox potentials by subtracting the Gibbs free energy of solvation ($\Delta G^\circ_{solv} = G^\circ_{aq.} - G^\circ_{gas}$) from the Gibbs free energy of the aqueous redox reaction ($\Delta G^\circ_{redox,aq.}$), arriving at $\Delta G^\circ_{gas} = E_{0\,K} + ZPE + \Delta\Delta G_{0\rightarrow 298\,K}$, where the first term is the energy at 0 K (from density functional theory at the optimum geometry), the second is the zero-point energies, and third, the thermal contributions, finally arriving at a ΔG°_{gas} and $E^0_{gasphase}$ from the Nernst equation ($E^0 = -\Delta G^\circ_{redox,aq.}/(nF)$).[45] In previous work, we demonstrated the MSR activity of a metal-oxide-based material: a zinc oxide (ZnO) catalyst with MeOH–water vapor with and without UV light and applied heat.[46] As seen in Fig. 2B, ambient temperature UV-assisted MSR and thermal MSR were not as favored as thermal + UV-light-assisted MSR. The analytical technique of electron paramagnetic resonance confirmed the production of UV-induced electrons and holes upon irradiation. The

electron reduces the Zn(II) to Zn(I), providing photogenerated holes for the MSR reaction. Other metal-oxide-based materials, such as CuO/ZnO in which a sputtered CuO layer was grown epitaxially on ZnO nanowires, showed the highest metal-oxide-based ESR activity at the time of the work (c. 2012).[47] Although the ZnO nanowire activity alone was not observed, the reaction conditions were considerably different (they were carried out in a homogeneous phase using 50 : 50 vol% water : EtOH under ambient conditions).

The benefit of using only ZnO is that it avoids the metallic Cu catalyst phase of the Cu/ZnO, which can be thermally sintered due to the hydroxylation of the ZnO phase. ZnO also exhibits H_2 heterolytic splitting, spillover, and recombination even at very low temperatures.[48] By using ZnO alone and allowing it to slowly hydroxylate, it is conceivable that the material could be reconditioned in a regeneration step to remove the water in the structure. Such a technique of operating two reactors in parallel (one online and one regenerating) is used throughout the chemical and petrochemical industries to recondition catalysts after deactivation.

Generally, a key aspect of photoreactor design and photochemistry is the consideration of isophotonic reactor volumes (like isothermal criteria for thermal reactors or thermochemistry), where a minimal gradient in the local volumetric rate of photon absorption is desirable. Kant and coworkers showed that for MeOH photoreforming with a photocatalyst composed of 0.025 wt% palladium on titania supported on an aerogel, complex relationships exist between temperature, photon rate of absorption (by varying photon flux), and feed concentration, which present optima for quantum yields (no. of production events over no. of absorbed photons).[49] Tuning these can, in turn, assist in maximizing the overall photocatalytic efficiency (no. of production events over no. of incident photons). As more researchers adopt these best practices, a deeper understanding and harnessing of photoreforming processes should result.

4.2 Feedstock options: MSR or DSR *vs.* fossil SMR as a hydrogen source

4.2.1 Challenge. There is a two-fold challenge to H_2 sourcing: (1) the need to find a favorable trade-off between FCV performance and durability, and (2) the cost of delivering acceptable quality H_2 to the consumer.[37] MSR and DSR are distinguished from SMR in that they avoid many shortfalls of the latter, as will be discussed here. Renewable production of MeOH and DME has been demonstrated at scale.[50] Methane can also be renewably sourced (such as from biogas *via* anaerobic digestion), although not at the scale needed for the H_2 economy.

4.2.2 MSR and DSR eliminate sulphur, ammonia, and inert gases, and are less complex overall than NG-fed SMR. MSR and DSR avoid sulphur compounds (such as H_2S) and NH_3 found naturally in fossil NG streams. Sulphur's effect on FCV catalysts requires it to be maintained at parts per billion (ppb) levels. Catalyst poisoning upon exposure to sulphur compounds has been found to increase with the duration of exposure. Like with sulphur, NH_3 poisoning is cumulative. The compound H_2S displaces CO (discussed in more detail later), even though the kinetics of CO are faster. This is due to the higher adsorptive strength of H_2S, which displaces CO over time, making

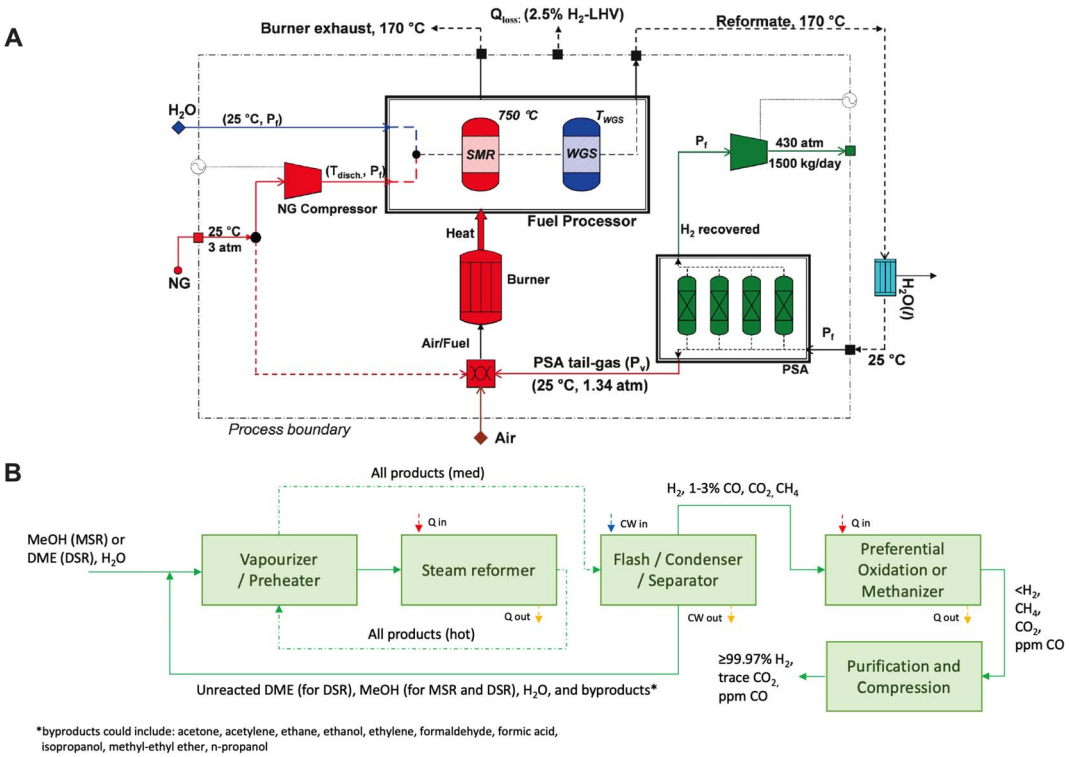

Fig. 3 Stationary reformer complexity and product H_2 purity requirements: (A) simplified schematic of the H_2 production-purification process for the SMR process from ref. 37, and (B) block diagram of equivalent stationary MSR or DSR, adapted from ref. 51.

durability and regenerability worse for the catalyst overall. The detection of sulfur compounds also requires 'extremely sensitive analytical equipment and careful monitoring of fuel quality along the entire fuel chain from production to dispensing'.[37]

MSR and DSR avoid inert helium and hydrocarbon contamination from dilute species present naturally in fossil NG streams. Helium is difficult to detect and can be present at 100 s of ppmv in NG. A cumulative inert amount of ~300 ppmv is recommended for FCV operation to avoid sensor and stack malfunction. SMR and water electrolysis both entrain gas contamination, such as air in the former and O_2 in the latter, which needs to be kept below certain thresholds (see Table 2).

Examples of SMR and MSR or DSR processes for H_2 are shown in Fig. 3A and B. Major differences are that the MSR or DSR can be operated at lower reforming temperatures of 200 °C to 300 °C compared to 750 °C for SMR. Both require WGS, water separation, pressure-swing absorption, or membrane separation, but liquid-fed MeOH or DME can be more easily compressed prior to the reforming step than NG.[35] A study highlighted that by operating the reformer at 5 bar instead of ambient pressure, the final energy requirement for compressing H_2 to 350 bar can be reduced by 30%.[38] A lower WGS step temperature in MSR or DSR is preferred due to more favorable CO conversion and thus is more compatible with the reforming temperature. Moderate pressures of 8 atm to 10 atm were modelled as good target pressures at a steam : carbon ratio of 4 for SMR, and similar results can be expected for MSR or DSR.[37]

4.2.3 MSR or DSR eases the removal of contaminants, attaining high H_2 gas quality. Table 2 shows the H_2 gas specification needed for current FCV durability, as mentioned previously. CO is seen as a limiting species to be removed, and higher CO removal leads to lower H_2 recovery and lower overall fuel efficiency. Maintaining a low CO concentration can affect the H_2 purity since N_2 can 'break through' in the PSA process if fed at high concentrations to this step. Because MSR or DSR feed a purer stream, they can be designed to avoid any entrained air during the process, which is an advantage of these routes. This highlights the challenge of maintaining all contaminants (He, HCs, O_2, water, N_2, Ar, *etc.*) at low-to-trace levels prior to PSA. CO_2 is easily removed from PSA.

Purification costs using PSA alone would be prohibitive for the purity requirements like the 0.2–10 ppmv CO (Table 2) for Pt anodes of FCVs. To address this, other methods for by-product removal that can be considered are the selective methanation of CO (SMC) or preferential oxidation (PROX) (Fig. 3B). SMC is an exothermic process that uses 2% Ru/γ-Al_2O_3 or Raney Nickel catalysts at conditions of 240 °C and 20 bar, whereby CO and CO_2 (with or without undergoing RWGS first) can be methanized with comparable activation energies (90 kJ mol^{-1} *vs.* 81 kJ mol^{-1}) and the unavoidable consumption of valuable H_2. Rahatade and coworkers found that >99.8% CO could be converted with ≤0.07% CO_2 for DSR with H_2 conversion around 10%.[51] MSR fared better than DSR in their analysis due to less product CO (1.5% *vs.* 2.5% absolute CO), converting only 6.8% of the H_2. Overall, the net present value of MSR-SMC *vs.* DSR-SMC was 1.9-fold better than that of DSR-SMC because of this and the significant utility cost savings of the former. PROX can, in addition, be used for on-board mobile reforming where CO is selectively and catalytically oxidized to CO_2. Allowing some CO_2 in the FCV feed, however, can cause ~20% loss in the maximum power density, and to compensate, higher flow rates can be used but can result in up to ~30% H_2 wastage.[52] Various platinum group metal and Au-based catalysts have been explored for PROX, and the catalyst requirements call for water stability and cost-effectiveness. Other catalyst requirements are facile O_2 splitting, avoidance of poisoning by –O or –OH groups, and lower oxidation barriers for CO compared to H_2.[53]

Maintaining strict CO specifications will increase the overall FCV efficiency (less fuel per km). In an analysis carried out by the U.S. DOE, assuming the relatively high H_2 fuels cost of ~US $ 4 per kg H_2, the CO purification only affected the H_2 cost by 4.4% over an order of magnitude change (0.1 ppmv to 100 ppmv CO).[37] However, when the U.S. DOE target for H_2 fuel cost at the station is US $ 1.5 per kg H_2, it may be necessary to optimize FCV stacks to be more durable to CO poisoning to lower gas cleanup requirements.

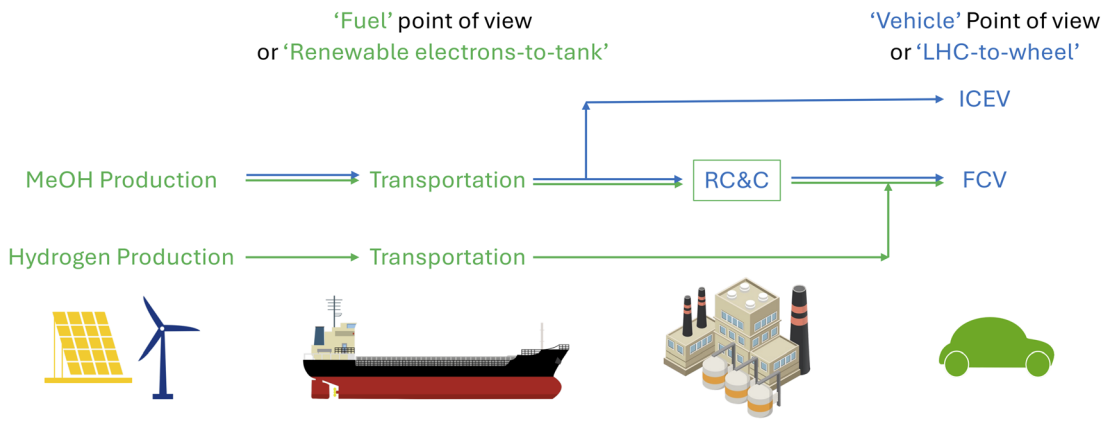

Fig. 4 Techno-economic analyses points of view to estimate the break-even RC&C cost. 'Vehicle' analysis considers the production and transportation identical up to local storage, and only the use case of renewable MeOH either as neat fuel for ICEVs or converted to H_2 for FCVs. 'Fuel' analysis considers the production and transport of MeOH or H_2 from the production source to the vehicle fuel tank.

5. Techno-economic analyses

5.1 Techno-economic analysis of renewable MeOH as drop-in fuel for ICEVs *vs.* reformed to H_2 for FCVs

Here, we detail two TEA: analysis (A) the 'vehicle' point of view, and analysis (B) the 'fuel' point of view as shown in Fig. 4. The goals of these two analyses are to attempt to quantify the break-even RC&C costs from two perspectives, namely, when using MeOH as a drop-in fuel *vs.* converted to H_2 and used in FCV (analysis A), and when comparing MeOH transport *vs.* gaseous and liquid H_2 transport (analysis B). MeOH can also be used as a drop-in fuel for ICEVs with few modifications at an assumed efficiency ($\eta_{eff,ICE}$) of 45% (due to its higher-octane rating) *vs.* 40% for gasoline, albeit with different and lower volumetric and gravimetric heating values. When considering the benefits of renewable fuels for drop-in ICEVs *vs.* FCVs, one should consider their total capital and operating costs including their GHG emissions. As shown in Fig. 5A, the capital cost outlays for road wear and gliders are similar for both types of vehicles. Currently, the drivetrain costs of FCVs are 8- to 9-fold higher (2018 Toyota Mirai US $ 174 per kW [55]) than the drivetrain of ICEVs (US $ 21 per kW [56]). FCV average engine costs by year for 2020, 2035, and 2050 are projected to be US $ 175, 60, and 30 kW^{-1}, respectively.[55] The cost of fuel supply in this analysis is assumed to be equivalent, supplied as renewable MeOH. As can be seen from this generalized representation in Fig. 5A, FCVs as of 2020 are more expensive than their ICEV counterparts without RC&C considerations over their lifetime, assuming no carbon tax. However, new benefits can be found with production economies of scale for the higher-efficiency FCV engines combined with their lower operating emissions by up to 56%, assuming 90 *vs.* 45% efficiency for FCV *vs.* ICEV and reasonable carbon tax scenarios. Although FCVs emit only water vapour as exhaust, when reconstituting the fuel H_2 fuel from the LHCs, the emissions are realized. However, due to the more efficient energy use, emissions are decreased by 56%. Then, the comparison becomes whether the combined costs of the drivetrain, fuel production emissions, and RC&C costs of useable H_2 can break even or become more affordable than ICEVs with their higher operating emissions. GHG emissions are assumed to be taxed at an ever-increasing amount in the future. The allowable share of LHC RC&C increases as the FCV drivetrain costs come down. As mentioned, FCV do not break even with ICEVs in 2020 until a carbon tax of at least $ US 50 per mt CO_2 is applied for an RC&C cost of ~US $ 0 per kg H_2. Because the addition of a reforming cost in 2020 (Fig. 5A) would already exceed the total drop-in MeOH ICEV cost (1 on the *x*-axis), there is no positive break-even RC&C cost that would work with this scenario; as such it is shown as US $ 0.0 per kW. RC&C costs are projected to contribute up to a maximum share of 0% to 53% of the TCO from 2020 to 2050 to break even with drop-in use, assuming all other costs remain fixed.

Fig. 5B shows how the carbon tax and drivetrain cost savings translate into a larger cost allowance for RC&C. These values represent the maximum RC&C cost that would allow FCVs to break even with a drop-in ICEV from 2020 to 2050. These were calculated by adding an operating carbon dioxide tax to the emissions cost, assuming an automobile engine size and lifetime of 62 kW and 250 000 km. Based on these figures, we calculated US $ per kW operating costs of US $ 0, 20.7, 34.4, 68.9, 172.2, and 344.3 per kW for the emissions of the ICEV/FCV for a few selected carbon tax values. As shown in Fig. 5B, the maximum RC&C cost will need to be between US $ 0.0 and US $ 7.8 per kg H_2 with aggressive carbon tax scenarios for inefficient fuel use of ICEVs. Currently, compressing H_2 accounts for US $ ~2.4 per kg H_2 at 700 bar pressure, leaving the upstream reforming and cleaning processes capital and operating budget at US $ <0–5.4 per kg H_2.[15] Realistically, it will be difficult for FCVs to compete cost-wise with drop-in ICEVs in 2035 and 2050 at low carbon tax incentives (≤US $ 50 per mt CO_2), where prices are US $ 2.9–3.6 per kg H_2 or at just about the compression costs. Global governments will need to significantly curb inefficient fuel use through higher carbon taxes for LHCs for FCVs to break even with LHCs for drop-in ICEV use.

5.2 Techno-economic analysis of liquid H_2 *vs.* renewable LHC-to-H_2 transport for FCVs

The previous section determined the maximum MeOH-to-H_2 RC&C cost when considering the ICEV and FCV capital and operation costs, but other operating costs can include fuel production, transport to exporting ports *via* pipeline, shipping,

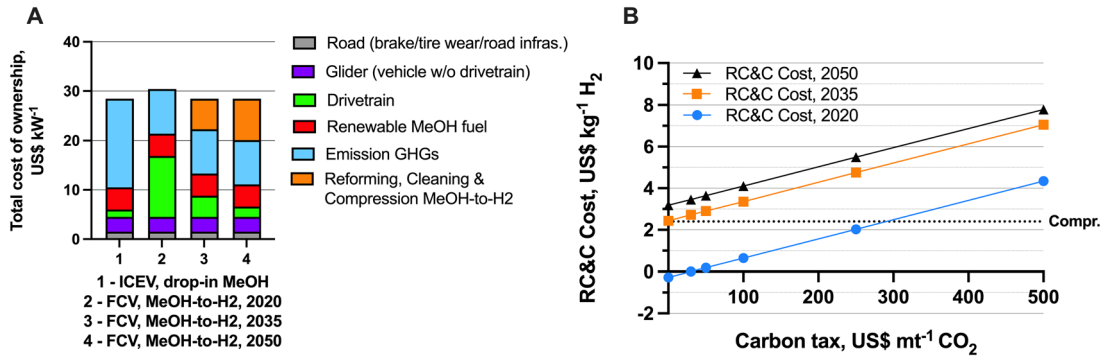

Fig. 5 (A) Vehicle costs in 2020, 2035, 2050 with $ US 0 per mt CO_2 carbon tax;[54] (B) RC&C cost with a carbon tax increase in 2020, 2035, and 2050 (see ESI† for the calculation method). The dotted line indicates the compression cost of H_2 to 700 bar at an average cost of $ US 2.3 per kg, as detailed in Table 3.

Table 3 Break-even RC&C cost for shipping-transporting LHCs compared to shipping gaseous-liquid H_2 (cost figures from ref. 15 and 34)[a]

Case	LHC (all for FCV, 80% fff. Unless stated otherwise)	H_2 price, US $ per kg H_2 (US $ per kg LHC)	Pipeline (US $ per kg H_2)	Comp./liq. (US $ per kg H_2)	Ship. (US $ per kg H_2)	Reform.-clean. (US $ per kg[1] H_2)	Comp. (At filling station) (US $ per kg H_2)	Distr. (To filling station) (US $ per kg H_2)	Total, (US $ per kg H_2)	Net H_2 to consumer\ (kg H_2)	Eff. kW h per kg H_2 (33.3 LHV H_2 basis)	Total eff., (US $ kW h^{-1})	Compare to case
(1)	MeOH – renewable	11.5 (1.45)	0.1	—	0.1	5.5	2.4	—	19.5	0.9	23.8	0.82	(9)
(2)	MeOH – renewable	11.5 (1.45)	0.1	—	0.1	9.0	2.4	—	23.0	0.9	23.8	0.97	(10)
(3)	MeOH – fossil	0.6 (0.3)	0.1	—	0.1	16.4	2.4	—	19.5	0.9	23.8	0.82	(9)
(4)	MeOH – fossil	0.6 (0.3)	0.1	—	0.1	19.9	2.4	—	23.0	0.9	23.8	0.97	(10)
(5)	MeOH – fossil	0.6 (0.3)	0.1	—	0.1	8.8	2.4	—	12.0	0.9	23.8	0.50	(11)
(6)	MeOH – renewable (ICEV, 45% eff.)	11.5 (1.45)	0.1	—	0.1	—	—	0.1	11.8	1.0	15.0	0.81	(9)
(7)	MeOH – fossil (ICEV, 45% eff.)	0.6 (0.3)	0.1	—	0.1	—	—	0.1	0.9	1.0	15.0	0.06	(11)
(8)	DME – renewable	20.1[b] (2.6)	0.1	—	0.1	0.4	2.4	—	23.1	0.9	23.8	0.97	(10)
(9)	H_2 (gas) – renewable	9.2	1.0	2.3 (comp)	4.0	—	—	3.0	19.5	0.9	23.8	0.82	(1), (3), (6)
(10)	H_2 (liq.) – renewable	9.2	1.0	4.0 (liq.)	2.3	—	—	1.5	18.0	0.7	18.6	0.97	(2), (4), (8)
(11)	H_2 (liq.) – fossil	0.6	1.0	4.0 (liq.)	2.3	—	—	1.5	9.4	0.7	18.6	0.50	(5), (7)

[a] US $ 1.0 per kg H_2 pipeline H_2 (ref. 15). US $ 0.01 per kg LHC transport (pipeline, ship, truck) LHC or ~US $ 0.1 per kg H_2 (ref. 15). US $ 0.1 to 4 per kg H_2 compression (700 bar)/liquefaction/storage H_2 (ref. 15). US $ 0.1 to 4 per kg H_2 transport H_2 ship (ref. 15). US $ 1.5 to 3 per kg H_2 compressed H_2 truck (ref. 15). Energy loss of LHV H_2 6% to 15% compression, LHV 18–30% liquefaction (ref. 4 and 15). Reform.-clean. and comp. columns combined are RC&C. [b] See ESI material for DME cost derivation.

and distribution to consumers. If transporting liquid H_2, then liquefaction needs to be considered prior to ship loading. Here, we assume only the costs for the fuel itself, which is the red bar in Fig. 5A.

Table 3 summarizes the various costs for producing, transporting, and distributing LHCs *vs.* pure H_2 for FCV use (eff. 80%). This 'fuel' cost accounting exercise is intended to show the maximum costs for RC&C of the LHC-derived H_2 to break-even with pure H_2 production and transport.

Renewable MeOH-to-H_2 for FCVs cannot currently (2020) compete with drop-in ICEV use (Case (6) in Table 3) when drivetrain costs are considered (previous section), and no option can compete from a cost standpoint with fossil MeOH drop-in use (Case (7) US $ 0.06 per kWh). As shown for renewable MeOH LHC (Cases (1) and (2)), the RC&C cost needs to be a maximum of US $ 7.9–11.4 per kg H_2 to break even with gaseous and liquid H_2 transport, respectively, in terms of useful motive energy. If fossil MeOH is used (Cases (3) and (4)) the RC&C cost is more flexible at US $ 18.8–22.4 per kg H_2 but would imply shortcomings of using a fossil fuel. Fossil MeOH (Case (5)) needs to be below a maximum RC&C cost of US $ 11.2 per kg H_2 to break even with fossil liquefied H_2. DME (Case (8)) was also included in this RC&C analysis and was found to require a very low US $ 2.8 per kg H_2 maximum cost to break-even with liquid H_2 (Case (10)), which may be only possible with lower-cost renewable electricity, longer-term storage, and stricter public safety and environmental considerations. The final delivered H_2 energy cost (including liquid H_2) remains about 6.5- to 10-fold higher compared to the U.S. DOE 'ultimate' threshold for delivered H_2 cost (US $ 0.08–0.12 per kWh). Closing this gap with LHCs can be realized by doing better than the break-even RC&C cost or producing the LHC more affordably compared to direct H_2. If the RC&C cost for Case (2) could achieve US $ 1 kg H_2, then it would become 3.9- to 6-fold the U.S. DOE ultimate target. As a final note, H_2 exhibits significant and varied boil-off during transportation and as such, to simplify the analysis, these detailed aspects were not considered. Detailed analysis of these aspects would consider shipping liquid H_2 overseas *via* tanker ship (4000 kg H_2)[15] as well as truck transport and storage, which can exhibit 0.3% and 1% to 5% H_2 losses per day, respectively. If these storage aspects were considered, it would have made the MeOH and DME RC&C costs more competitive. For comparison, a 2022 study by Collis and Schomäcker found for green H_2 production plus transport costs, with the H_2 carrier for the latter in the form of H_2 gas, H_2 liquid, ammonia, or toluene to be between $ US 9.9–17.9 per kg H_2, in the same magnitude as derived here $ US 9.4–23.1 per kg H_2.[57]

In our previous work, we detailed the production of a solar-MeOH LHC, consisting of direct-air-captured (DAC) CO_2 and green H_2, and our follow-up studies detailed ways to lower the renewable MeOH MSP with low-temperature thermal catalyst improvements or photocatalysis.[34,58] We determined *via* TEA that the price can vary from US $ 1.41 (Strategy A1 (ref. 58)) to 1.45 per kg MeOH (Strategy A[34]), or about 5-fold the fossil price, which is included in the Table 3 analysis. The direct-air-capture cost of CO_2 was assumed to be $ US 51 per mt CO_2, in line with

the order of magnitude outlook of the United States Government 45Q tax credits.[34] Schorn *et al.*[4] carried out an analysis of the CO_2 capture cost in the origin and destination countries, a similar analysis to the RC&C costs considered herein. They found that as long as the CO_2 direct air capture costs are cheaper than the added expense of H_2 transport than transporting LHCs makes more sense. They found for a MeOH LHC, a break-even CO_2 capture cost of US$ 197–248 per mt CO_2 was needed, which should be readily achievable at scale. In a new paradigm, Schühle and coworkers proposed the idea of a closed DME/CO_2 storage and release cycle, whereby CO_2 is captured at the destination and returned to the source, lowering delivered H_2 costs by 26–56% depending on whether current or future DAC costs are used. In their comprehensive analysis, DME/CO_2 is shown to be preferential compared to MeOH and ammonia from either a materials compatibility and water demand point of view, or an energy demand and net-H_2 point of view, respectively.[26] DME in their view has a bright future as an efficient and safe LHC option.

6. Conclusions

As evidenced by proposed international projects, LHCs such as methane, ammonia, MeOH, and DME will remain critical to transport H_2 across global distances to existing population centers. The TEA presented herein for MeOH and DME LHCs shows that their combined RC&C cost percentage cannot exceed 0–53% of the total cost of ownership of FCVs to be cost-effective *vs.* drop-in ICEVs in 2020 to 2050 scenarios. On a lifetime cost basis, the MSR RC&C costs need to fall below US $ 0.0–3.18 per kg H_2 without carbon taxes, US $ 0.64–4.10 per kg H_2 with intermediate carbon taxes (~US $ 100 per mt CO_2) and US $ 4.34–7.79 per kg H_2 with aggressive carbon taxes (US $ 500 per mt CO_2) to compete with drop-in use. For MeOH fuel production, distribution, and conversion to H_2 fuel costs to break even with gaseous or liquid H_2 transport, the MSR RC&C cost is a flexible US $ 7.9–11.4 per kg H_2 without carbon tax incentives. DME is interesting as a safe, user-friendly, and environmentally friendly alternative to MeOH but requires more energy to produce, which results in a nearer break-even final H_2 cost compared to gaseous and liquid H_2 transport. LHCs look favorable compared to pure H_2 transport in all scenarios; however, centralized LHC economies-of-scale RC&C is needed to drive this steps' costs down to compete with drop-in alternatives.

Abbreviations

LHC	liquid hydrogen carrier
H_2	molecular hydrogen
MeOH	methanol
MSR	methanol steam reforming
DME	dimethyl ether
DSR	dimethyl ether steam reforming
RC&C	reforming, cleaning, and compression
SMR	steam-methane reforming
FCVs	proton-exchange membrane fuel-cell vehicles
ICEVs	internal combustion engine vehicles
'Ultimate'	a U.S.DOE term for a future best-case scenario
Gge	gallon of gasoline equivalent
CO	carbon monoxide
(R)WGS	(reverse) water gas shift
mt	metric tonnes
TEA	techno-economic analysis

Data availability

The data supporting this article have been included as part of the ESI.†

Author contributions

A. A. T. carried out the methodology, investigation and wrote the paper. All authors conceived, visualized, acquired funding for, reviewed, and edited the paper.

Conflicts of interest

There are no conflicts to declare.

Acknowledgements

All authors thank Keshav Raina for proofreading the manuscript. We thank the Mitacs Accelerate Grant and Ford Motor Canada for financial support since Sept. 2022. We also acknowledge Hydrofuel Canada Inc. for financial support since June 2023. Fig. 4 clip art courtesy of j4p4n, Firkin, dominiquechappard, and TVLuke from website **https://openclipart.org**.

Notes and references

1 Hydrogen Fuel Technology: a Cleaner and More Secure Energy Future, 2003, available from: **https://georgewbush-whitehouse.archives.gov/infocus/technology/economic_policy200404/chap2.html**.

2 A. Kampker, H. Heimes, B. Dorn, D. Neb, H. Clever and J. Machura. Conference on Production Systems and Logistics Cpsl 2023-2 5 th Conference on Production Systems and Logistics Hype Cycle Assessment Of Emerging Technologies For Battery Production, available from, DOI: **10.15488/15220**.

3 A. A. Tountas, G. A. Ozin and M. M. Sain, Solar methanol energy storage, *Nat. Catal.*, 2021, **4**(11), 934–942.

4 F. Schorn, J. L. Breuer, R. C. Samsun, T. Schnorbus, B. Heuser, R. Peters, *et al.*, Methanol as a renewable energy carrier: An assessment of production and transportation costs for selected global locations, *Adv. Appl. Energy*, 2021, **3**, 100050.

5 BNN Bloomberg, *Morocco Seeks Partners to Build Gas and Green Hydrogen Network*, 2023, available from: **https://**

www.bnnbloomberg.ca/morocco-seeks-partners-to-build-gas-and-green-hydrogen-network-1.1973967.
6 Reuters, *Hyphen and Namibia Agree Next Phase of $10 Billion Green Hydrogen Project*, 2023, available from: https://www.reuters.com/business/energy/hyphen-namibia-agree-next-phase-10-bln-green-hydrogen-project-2023-05-24/.
7 Voice of America News, *Namibia Signs $10 Billion Green Energy Deal with Germany's Hyphen*, 2023, available from: https://www.voanews.com/a/namibia-signs-10-billion-green-energy-deal-with-germany-s-hyphen-/7118163.html.
8 K. C. Ott, T. Autrey and F. Stephens, *Final Report for the DoE Chemical Hydrogen Storage Center of Excellence; LA-UR-20074*, 2012.
9 J. G. Speight, Chapter 8 - Hydrocarbons from synthesis gas, in *Handbook of Industrial Hydrocarbon Processes*, ed. J. G. Speight, Gulf Professional Publishing, Boston, 2nd edn, 2020, pp. 343–386, available from: https://www.sciencedirect.com/science/article/pii/B9780128099230000084.
10 M. Konsolakis, Z. Ioakimidis, T. Kraia and G. E. Marnellos, Hydrogen production by ethanol steam reforming (ESR) over CeO2 supported transition metal (Fe, Co, Ni, Cu) catalysts: Insight into the structure-activity relationship, *Catalysts*, 2016, **6**(39), 1–27.
11 F. A. Elewuwa and Y. T. Makkawi, Hydrogen production by steam reforming of DME in a large scale CFB reactor. Part I: Computational model and predictions, *Int. J. Hydrogen Energy*, 2015, **40**(46), 15865–15876https://www.sciencedirect.com/science/article/pii/S0360319915025367.
12 D. S. Newsome, The Water-Gas Shift Reaction, *Catal. Rev.*, 1980, **21**(2), 275–318, DOI: 10.1080/03602458008067535.
13 Nationaler Wasserstoffrat, *The (National Hydrogen Council) Hydrogen Transport July 2021*, 2021, available from: https://wasserstoffwirtschaft.sh/file/nwr_wasserstofftransport_web-bf.pdf.
14 Hydrogen and Fuel Cell Technologies Office, *Hydrogen Pipelines*, 2023, available from: https://www.energy.gov/eere/fuelcells/hydrogen-pipelines.
15 P. T. Aakko-Saksa, C. Cook, J. Kiviaho and T. Repo, Liquid organic hydrogen carriers for transportation and storing of renewable energy – Review and discussion, *J. Power Sources*, 2018, **396**(July), 803–823.
16 D. Li, X. Li and J. Gong, Catalytic Reforming of Oxygenates: State of the Art and Future Prospects, *Chem. Rev.*, 2016, **116**(19), 11529–11653.
17 T. A. Semelsberger and R. L. Borup, Thermodynamics of Hydrogen Production from Dimethyl Ether Steam Reforming and Hydrolysis, *Thermodynamics of Hydrogen Pro- Duction from Dimethyl Ether Steam Reforming and Hydrolysis*, 2004;LA-14166.
18 P. Kevin, M. Julio and G. Andrew, *North America Midstream Infrastructure through 2035*, 2018, vol. 120.
19 International Energy Agency, *Putting CO2 to Use. Energy Report*, 2019, p. 86.
20 United States Environmental Protection Agency, *Global Greenhouse Gas Overview*, 2024, [cited 2024 Jul 29], available from: https://www.epa.gov/ghgemissions/global-greenhouse-gas-overview.
21 F. Xiao, Q. Wang, G. L. Xu, X. Qin, I. Hwang, C. J. Sun, *et al.*, Atomically dispersed Pt and Fe sites and Pt–Fe nanoparticles for durable proton exchange membrane fuel cells, *Nat. Catal.*, 2022, **5**(6), 503–512.
22 U.S. DRIVE Partnership, *Hydrogen Storage Tech Team Roadmap*, 2017, p. 59.
23 K. C. Christoforidis and P. Fornasiero, Photocatalytic Hydrogen Production: A Rift into the Future Energy Supply, *ChemCatChem*, 2017, **9**(9), 1523–1544.
24 Technical Targets for Proton Exchange Membrane Electrolysis - Hydrogen and Fuel Cell Technologies Office, 2023, available from: https://www.energy.gov/eere/fuelcells/technical-targets-proton-exchange-membrane-electrolysis.
25 DOE Technical Targets for Hydrogen Delivery - Hydrogen and Fuel Cell Technologies Office, 2023, available from: https://www.energy.gov/eere/fuelcells/doe-technical-targets-hydrogen-delivery.
26 P. Schühle, R. Stöber, M. Semmel, A. Schaadt, R. Szolak, S. Thill, *et al.*, Dimethyl ether/CO2 - a hitherto underestimated H2 storage cycle, *Energy Environ. Sci.*, 2023, **16**(7), 3002–3013.
27 P. Preuster, C. Papp and P. Wasserscheid, Liquid organic hydrogen carriers (LOHCs): Toward a hydrogen-free hydrogen economy, *Acc. Chem. Res.*, 2017, **50**(1), 74–85.
28 M. D. Masekameni, R. Moolla, M. Gulumian and D. Brouwer, Risk Assessment of Benzene, Toluene, Ethyl Benzene, and Xylene Concentrations from the Combustion of Coal in a Controlled Laboratory Environment, *Int. J. Environ. Res. Public Health*, 2018, **16**(1), 95.
29 D. J. Drury, Formic Acid, in *Kirk-Othmer Encyclopedia of Chemical Technology*, John Wiley & Sons, Ltd, 2000.
30 P. Rosha, A. Jelle and H. Ibrahim, Recent advances in hydrogen production through catalytic steam reforming of ethanol: Advances in catalytic design, *Can. J. Chem. Eng.*, 2023, 1–21.
31 *How to Spend $50 Billion to Make the World a Better Place*, ed. B. Lomborg, Cambridge University Press, Cambridge, 2006, pp. 175–183.
32 S. Michailos, S. McCord, V. Sick, G. Stokes and P. Styring, Dimethyl ether synthesis via captured CO2 hydrogenation within the power to liquids concept: A techno-economic assessment, *Energy Convers. Manag.*, 2019, **184**(January), 262–276.
33 U.S. Energy Information Administration, *How Much Electricity Does an American Home Use?*, 2021, available from: https://www.eia.gov/tools/faqs/faq.php?id=97&t=3#:~:text=In2021theaverageannual,about886kWhpermonth.
34 A. A. Tountas, X. Peng, A. V. Tavasoli, P. N. Duchesne, T. L. Dingle, Y. Dong, *et al.*, Towards Solar Methanol: Past, Present, and Future, *Advanced Science*, 2019, **6**(8), 1–52.
35 S. Sahebdelfar and M. T. Ravanchi, Carbon monoxide clean-up of the reformate gas for PEM fuel cell applications: A conceptual review, *Int. J. Hydrogen Energy*, 2022, **48**(64), 24709–24729.

36 K. Arrhenius, A. Alexandersson, H. Yaghooby, J. Engelbrektsson and N. Stromberg, Analysis of hydrogen quality, *Teknikbevakning Bransleceller*, 2015.
37 U.S. Department of Energy, J. M. Ohi, N. Vanderborgh and G. Voecks. Hydrogen Fuel Quality Specifications for Polymer Electrolyte Fuel Cells in Road Vehicles, *Safety, Codes and Standards Program*, 2016, pp. 1–72.
38 E. Gapp and P. Pfeifer, Membrane reactors for hydrogen production from renewable energy sources, *Current Opinion in Green and Sustainable Chemistry*, Elsevier B.V., 2023, vol. 41.
39 K. Kappis, J. Papavasiliou and G. Avgouropoulos, *Methanol Reforming Processes for Fuel Cell Applications*, 2021, vol. 1–30.
40 A. A. Tountas, G. A. Ozin and M. M. Sain, Continuous reactor for renewable methanol, *Green Chem.*, 2021, **23**(1), 340–353.
41 Y. H. Chin, R. Dagle, J. Hu, A. C. Dohnalkova and Y. Wang, Steam reforming of methanol over highly active Pd/ZnO catalyst, *Catal. Today*, 2002, **77**(1–2), 79–88.
42 A. B. Patil, B. D. Jadhav and P. V. Bhoir, Efficient photocatalytic hydrogen production over Ce/ZnO from aqueous methanol solution, *Mater. Renew. Sustain. Energy*, 2021, **10**(4), 1–9.
43 H. Ahmad, S. K. Kamarudin, L. J. Minggu and M. Kassim, Hydrogen from photo-catalytic water splitting process: A review, *Renew. Sustain. Energy Rev.*, 2015, **43**, 599–610.
44 A. Wang, A. A. Tountas and G. A. Ozin, Bringing down the heat in methanol synthesis, *Matter*, 2023, 1–30.
45 J. Moens, P. Geerlings and G. Roos, A conceptual DFT approach for the evaluation and interpretation of redox potentials, *Chem.—Eur. J.*, 2007, **13**(29), 8174–8184.
46 A. A. Tountas, *Solar Methanol: from Process Engineering and Photoreactor Development to Materials Discovery and Photocatalysis*, PhD thesis, University of Toronto, 2021.
47 Q. Simon, D. Barreca, A. Gasparotto, C. MacCato, T. Montini, V. Gombac, *et al.*, Vertically oriented CuO/ZnO nanorod arrays: From plasma-assisted synthesis to photocatalytic H2 production, *J. Mater. Chem.*, 2012, **22**(23), 11739–11747.
48 H. Shi, H. Yuan, Z. Li, W. Wang, Z. Li and X. Shao, Low-Temperature Heterolytic Adsorption of H2 on ZnO(1010) Surface, *J. Phys. Chem. C*, 2019, **123**(21), 13283–13287.
49 P. Kant, L. L. Trinkies, N. Gensior, D. Fischer, M. Rubin, G. A. Ozin, *et al.*, Isophotonic reactor for the precise determination of quantum yields in gas, liquid, and multi-phase photoreactions, *Chem. Eng. J.*, 2023, **452**(P2), 139204.
50 J. Williams, *Oberon Fuels Starts Commercial Production of Renewable Dimethyl Ether (rDME), a Pivotal Step towards a Net-Zero Future*, 2021, available from: **https://oberonfuels.com/2021/06/10/oberon-fuels-starts-commercial-production-of-renewable-dimethyl-ether-rdme-a-pivotal-step-towards-a-net-zero-future/**.
51 S. S. Rahatade and N. A. Mali, Techno-economic assessment of hydrogen production via dimethylether steam reforming and methanol steam reforming, *Indian Chem. Eng.*, 2023, 1–17.
52 A. Iulianelli, P. Ribeirinha, A. Mendes and A. Basile, Methanol steam reforming for hydrogen generation via conventional and membrane reactors: A review, *Renew. Sustain. Energy Rev.*, 2014, **29**(February 2015), 355–368.
53 Y. Xi and A. Heyden, Preferential Oxidation of CO in Hydrogen at Nonmetal Active Sites with High Activity and Selectivity, *ACS Catal.*, 2020, **10**(9), 5362–5370.
54 A. Simons and C. Bauer, A life-cycle perspective on automotive fuel cells, *Appl. Energy*, 2015, **157**, 884–896.
55 M. M. Whiston, I. M. Lima Azevedo, S. Litster, C. Samaras, K. S. Whitefoot and J. F. Whitacre, Expert elicitation on paths to advance fuel cell electric vehicles, *Energy Pol.*, 2022, **160**(55), 112671.
56 Z. Liu, J. Song, J. Kubal, N. Susarla, K. W. Knehr, E. Islam, *et al.*, Comparing total cost of ownership of battery electric vehicles and internal combustion engine vehicles, *Energy Pol.*, 2021, **1**, 158.
57 J. Collis and R. Schomäcker, Determining the Production and Transport Cost for H2 on a Global Scale, *Front. Energy Res.*, 2022, **10**, 1–27.
58 A. A. Tountas, X. Peng, Y. Xu, R. Song, L. Wang, C. T. Maravelias, *et al.*, Direct CO2-to-renewable methanol: Outlook, performance and optimization approach, *Sustainable Mater. Technol.*, 2023, **36**(March), e00630.

